Electronic Supplementary Information

Electronic structures and enhanced photocatalytic properties of blue phosphorene/BSe van der Waals heterostructures

Bao-Ji Wang,[a] Xiao-Hua Li,[a] Ruiqi Zhao,[*b] Xiao-Lin Cai,[a] Wei-Yang Yu,[a] Wei-Bin Li,[a] Zhen-Shen Liu,[a] Li-Wei Zhang,[a] and San-Huang Ke[*c]

[a]School of Physics and Electronic Information Engineering, Henan Polytechnic University, Jiaozuo 454000, China

[b]School of Materials Science and Engineering, Henan Polytechnic University, Jiaozuo 454000, China

[c]MOE Key Laboratory of Microstructured Materials, School of Physics Science and Engineering, Tongji University, Shanghai 200092, China

*Corresponding authors: zhaoruiqi@hpu.edu.cn; shke@tongji.edu.cn

1. Schematic structures of stable homo-bilayers of BlueP and BSe.
2. Phonon spectra of BlueP/BSe heterobilayers with different stacking sequences.
3. Comparison of band structures and electrostatic potentials obtained with/without dipole corrections.
4. Side views of the stable multilayer heterostructures.
5. Projected band structures of the multilayer heterostructures with stable stacking sequence.
6. The band edge alignments of multilayered heterostructures.

1. Schematic structures of stable homo-bilayers of BlueP and BSe.

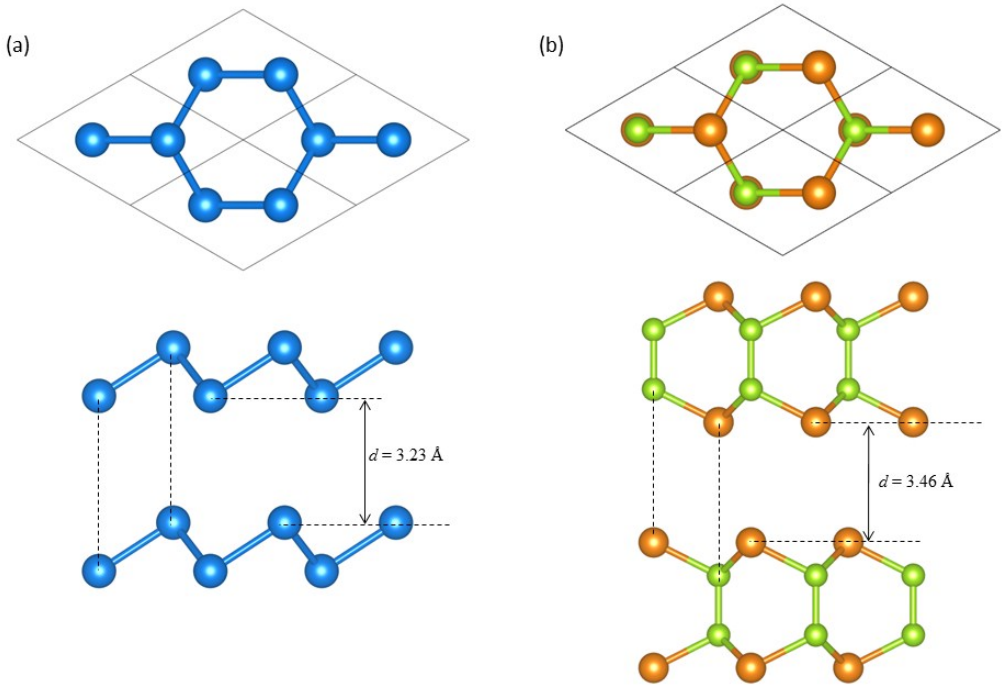

Fig. S1. Top and side views of homo-bilayers of (a) BlueP and (b) BSe. Bilayer BlueP favors AA-stacked pattern [1] while bilayer BSe prefers β-type structure (being similar to bilayer GaS [2, 3]), which can be verified by comparing the total energies of the homo-bilayer with different stacking forms. The arrows indicate the inter-layer distance *d* between homo-bilayers.

2. Phonon spectra of BlueP/BSe heterostructures with different stacking sequences.

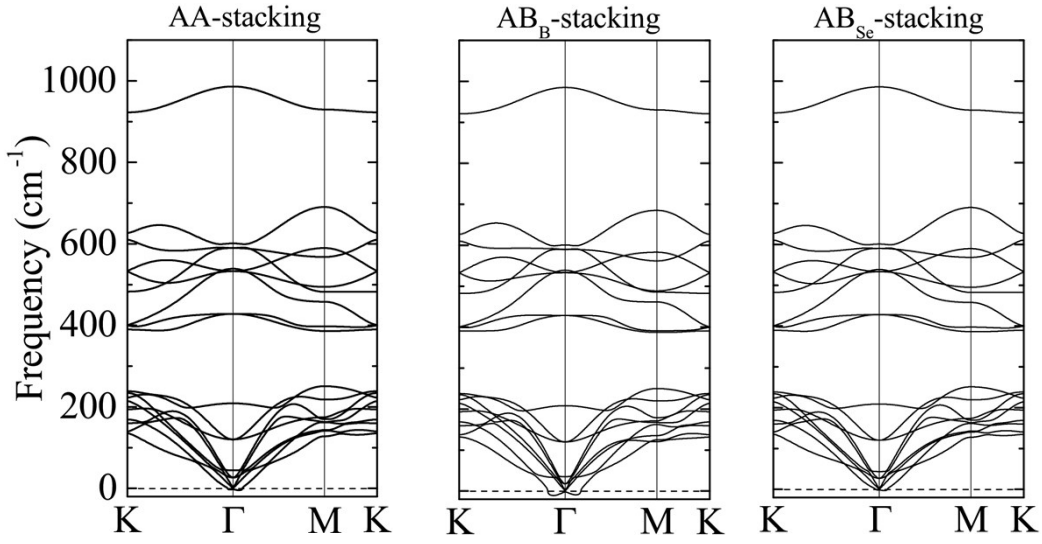

Fig. S2. Phonon dispersion curves of BlueP/BSe heterostructures stacked in AA-, AB_B- and AB_{Se} sequences.

3. Comparison of band structures and electrostatic potentials obtained with/without dipole corrections.

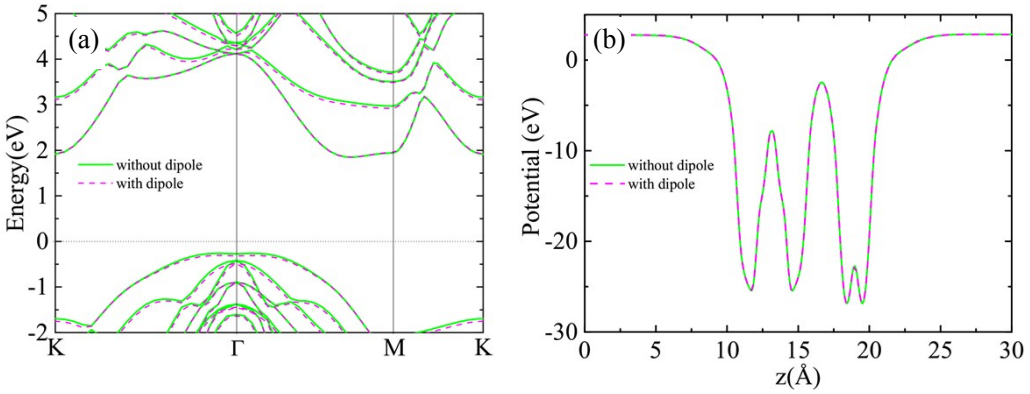

Fig. S3. (a) Band structures and (b) electrostatic potentials of AA-stacked BlueP/BSe heterostructure obtained with/without dipole corrections. All results are calculated with HSE06 functional.

4. Side views of the stable multilayer heterostructures.

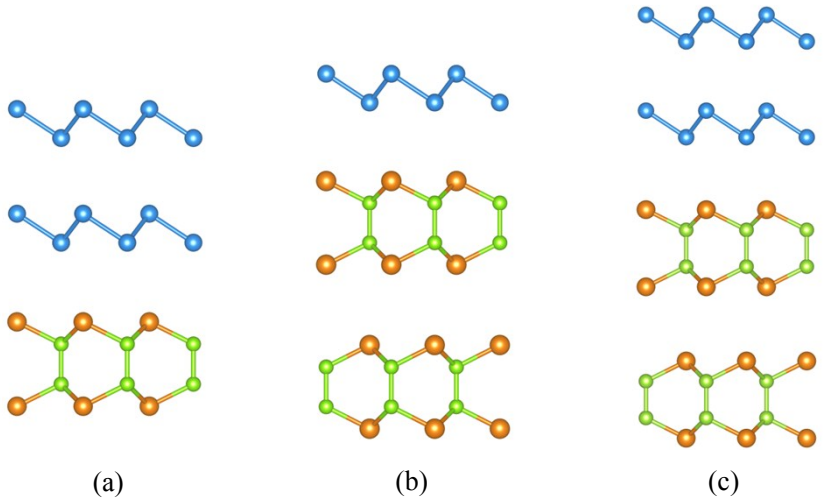

Fig. S4. Side views of the stable multilayer heterostructures: (a) 2L-BlueP/BSe, (b) BlueP/2L-BSe, (c) 2L-BlueP/2L-BSe. Here, the stacking in homo-subbilayers is consistent with that shown in Fig. S1 while that of heterobilayers takes the AA-stacking form, being the same as the stable configuration of the heterostructure discussed in the main text.

5. Projected band structures of the multilayer heterostructures with stable stacking sequence.

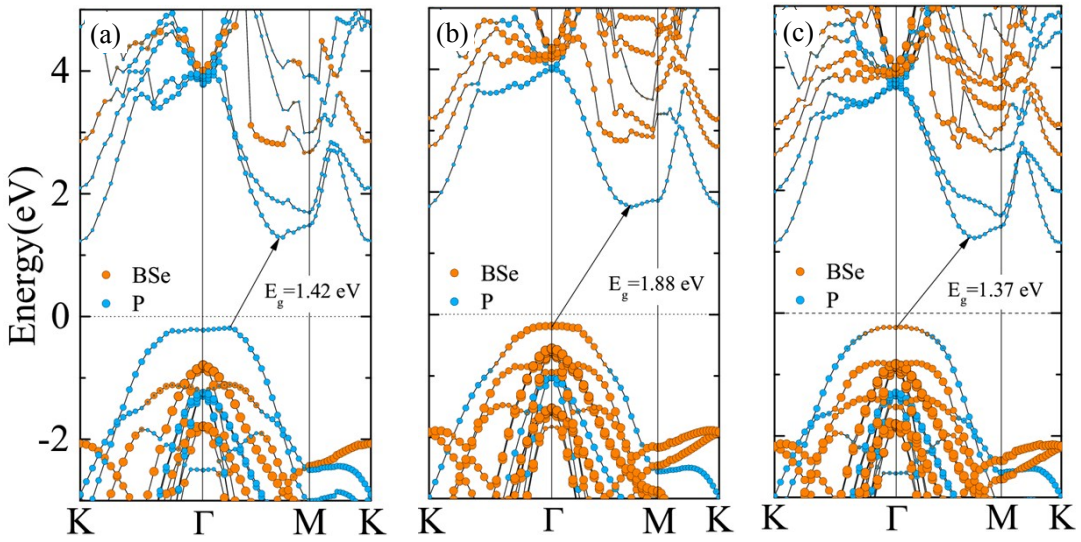

Fig. S5. Projected band structures of the multilayer heterostructures with stable configuration: (a) 2L-BlueP/BSe, (b) BlueP/2L-BSe, (c) 2L-BlueP/2L-BSe. The results are calculated by HSE06 functional.

6. The band edge alignments of multilayered heterostructures.

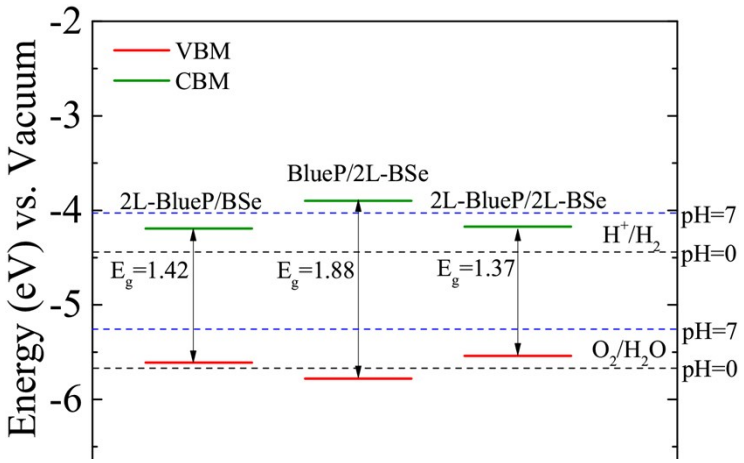

Fig. S6. The band edge alignments of 2L-BlueP/BSe, BlueP/2L-BSe, 2L-BlueP/2L-BSe multilayer heterostructures relative to the vacuum level. The oxidation (O_2/H_2O) and reduction (H^+/H_2) potentials of water splitting at pH = 0 (black dashed line) and pH = 7 (blue dashed line) are shown for comparison.

References

[1] B. Ghosh, S.Nahas, S.Bhowmick and A.Agarwal, *Phys. Rev. B*, 2015, **91**, 115433.

[2] Z. Zhu, Y. Cheng and U. Schwingenschlögl, *Phys. Rev. Lett.*, 2012, **108**, 266805.

[3] Y. Ma, Y. Dai, M. Guo, L. Yu and B. Huang, *Phys. Chem. Chem. Phys.*, 2013, **15**, 7098.